# $^{11}$B NMR and relaxation study of boron nitride

M. Fanciulli*
*Department of Physics, Boston University, Boston, Massachusetts 02215*

M. Corti
*Department of Physics "A. Volta," University of Pavia, 27100 Pavia, Italy*
(Received 23 December 1993; revised manuscript received 7 June 1995)

The different allotropic forms of boron nitride have been investigated by $^{11}$B NMR and spin-lattice relaxation measurements. In the material with hexagonal symmetry the central transition is broadened by second-order quadrupole perturbation and the related quadrupole frequency $\nu_Q = e^2qQ/2h$ is found to be 1.50±0.05 MHz, a result interpreted on the basis of charge transfer from B to N. The study of the $^{11}$B spin-lattice relaxation shows that the dominant mechanism is related to the presence of paramagnetic centers, i.e., nitrogen vacancies, previously investigated by electron paramagnetic resonance. The relaxation mechanism due to lattice vibrations is relevant only in samples with a very low concentration of paramagnetic centers. An analysis of temperature and field dependences of the magnetic relaxation rates is carried out in terms of the competing processes of spin-diffusion-driven and electronic-relaxation-driven mechanisms. Enlightening information on the relaxation regimes and the spin dynamics of the paramagnetic centers is obtained from a comparison of the experimental findings with the theoretically expected behaviors.

## I. INTRODUCTION

Boron nitride is a wide band-gap semiconductor with interesting properties from both physical and technological points of view. Bulk BN shows a polymorphism similar to carbon, crystallizing in the hexagonal (graphitelike) and in the zinc-blende structure. Due to the difference in electronegativity between B and N, a significant charge transfer from the B atom to the N atom is present.[1] Thus BN can be considered a polar material, and this yields the differences with respect to the related carbon structures. Hexagonal BN (*h*-BN) is a semiconductor with an indirect gap $E_g = 3.9$ eV (Ref. 2) and $D^4_{6h}$ symmetry. Graphite, a semimetal, is isoelectronic to *h*-BN, but the stacking arrangement of the layers is different. Favored by the Coulomb attraction, B and N atoms are stacked directly over each other, in consecutive layers. The zinc-blende structure (*c*-BN), synthesized in 1957 (Ref. 3), has an indirect gap $E_g = 6.4$ eV (Ref. 4) and a lattice of $T^2_d$ symmetry. Properties such as extreme hardness and high melting point as well as interesting dielectric, thermal, and optical characteristics lead to several potential uses for *c*-BN, involving electronic, optoelectronic, and coating applications. Reviews of the structural and electronic properties of BN have been published by Paine and Narula[5] and by Galikova.[6] Preparation, properties, and applications of BN thin films have been reviewed by Arya and D'Amico,[7] while a general overview on the device implementations of wide band-gap semiconductors has been published by Edgar.[8]

Early $^{11}$B NMR measurements had been performed on hexagonal boron nitride by Silver and Bray,[9] and from the quadrupole coupling constant information on the bonding electrons was extracted. To the author's knowledge, no measurements of nuclear relaxation rates, either in "quasipure" BN or in samples with paramagnetic centers, have been reported until now. It is noteworthy that paramagnetic defects are present in all BN structures[10–17] and they can affect several important properties. The dominant center is the nitrogen vacancy with an electron trapped therein, such as *F* centers in alkali halides.[12,13] The samples have been analyzed also by electron paramagnetic resonance (EPR) (Refs. 15–17) and a study of the electron spin-relaxation properties of the paramagnetic defect has recently been published.[17] In this paper we report the results of a $^{11}$B NMR study of bulk polycrystalline *c*-BN (prepared by high-pressure and -temperature methods), pyrolitic *h*-BN, and thin films prepared by reactive sputtering. From the second-order electric quadrupole perturbation effects, information on the electric-field gradients (EFG) at the nuclear site is derived. $^{11}$B spin-lattice relaxation measurements, carried out in the temperature range 4–300 K and for two values of the external magnetic field, are related to the dynamics of the paramagnetic centers, and insights on their spin-lattice relaxation and spin-diffusion process are obtained.

## II. EXPERIMENTAL DETAILS

The BN films were grown by reactive rf sputtering from a hexagonal boron nitride target in an atmosphere containing a mixture of argon and nitrogen (total pressure $P_t = 2$ mTorr, $P_{N_2} = 10\%$, power $P = 1250$ W). The boron nitride target was Carborundum grade AX20, which contains 2% $B_2O_3$. Films for this study were deposited on silicon (100) substrates (substrate temperature $T_s = 550$ °C) and self-supporting samples were obtained by

 

dissolving the substrate in a solution containing HF and $HNO_3$. Details on the growth technique and sample characterization have been reported elsewhere.[15–18] As reference for the hexagonal BN the same material of the target has been used, while two different cubic-BN samples have been studied; the General Electric Borazon (GE/Borazon 80% *c*-BN+20% TiN, powder size 0.5 $\mu$m) and the translucent *c*-BN produced by Sumitomo Electric (resistivity $10^{11}$–$10^{12}$ $\Omega$ cm, polycrystalline). The NMR measurements were performed by means of a BRUKER MSL 200 Fourier transform (FT) pulse spectrometer, mostly at $H_0 \simeq 5.9$ and 1.6 T, corresponding to the measuring frequencies $\nu_L = 80.47$ and 21.8 MHz, respectively.

The spectra have been obtained by FT of the free induction decay (FID) following a $\pi/2$ rf pulse or from FT of half of the echo signal generated by a $\pi/2$-$\tau$-$\pi$ pulse sequence. The spin-spin dephasing time $T_2$ was derived from the amplitude of the echo signal as a function of the time $\tau$ between the two rf pulses.

The $^{11}$B nuclear spin-lattice relaxation was studied by monitoring the echo intensity $m(t)$ as a function of the time $t$ after a saturation sequence. The relaxation rate $W$'s were extracted from the behavior of the recovery law $y(t)=[m(\infty)-m(t)]/m(\infty)$. The relation expressing $y(t)$ in terms of $W$ can be found by solving the master equations for the populations $N_m(t)$ of the Zeeman levels, in correspondence to the appropriate initial conditions induced by the saturating rf pulses (see Sec. IV A).

## III. $^{11}$B NUCLEAR QUADRUPOLE COUPLING — RESULTS AND DISCUSSION

The spin Hamiltonian for the $^{11}$B nucleus in BN with paramagnetic centers is

$$\mathcal{H} = -\hbar g_N \beta_N H_0 I_z + [e^2qQ/4I(2I-1)][3I_z^2 - I^2 + \eta(I_x^2 - I_y^2)] + \mathcal{H}_{\text{dip}} + \mathcal{H}_{e\text{-}n} , \quad (1)$$

where the first term is the nuclear Zeeman interaction with the external magnetic field $\mathbf{H}_0 \| \mathbf{z}$, and the second term describes the quadrupolar interaction of the EFG, $eq = V_{zz}$ being the largest principal value; $eQ$ is the nuclear electric quadrupole moment; $\eta$ is the asymmetry parameter $\eta = (V_{xx} - V_{yy})/V_{zz}$, with $|V_{zz}| \geq |V_{yy}| \geq |V_{xx}|$. In Eq. (1) $\mathcal{H}_{\text{dip}}$ represents the dipolar interaction between the $^{11}$B nuclei and the other nuclei in the system, and $\mathcal{H}_{e\text{-}n}$ represents the interaction between the nuclear magnetic moment and an effective magnetic moment of the center, through the dipolar and contact interactions.

The last two terms do not contribute significantly to the spectra; they are, however, important for the relaxation processes. The nuclear quadrupole interaction can be treated as a perturbation of the Zeeman Hamiltonian. To first order the frequency of the central line, related to the transition between the $m = \frac{1}{2}$ and $-\frac{1}{2}$ states, is not changed. In a single crystal the satellite lines ($\pm\frac{3}{2} \leftrightarrow \pm\frac{1}{2}$ transitions) would be shifted by an amount given by $\nu_Q = e^2qQ/2h$ times an angular function related to the orientation of the magnetic field in the EFG principal-axis frame of reference. Thus in a powder the satellite lines are distributed over a frequency range of the order of $2\nu_Q$, with weak singularities at $\pm\nu_Q/2$ that are difficult to detect. In our samples, due to the low sensitivity at small field and possibly to a distribution of EFG, it turned out to be impractical to derive the strength of the quadrupole interaction from the singularities of the satellite lines. The broadening of the central line due to the powder distribution of the second-order quadrupole perturbation was used instead.

For trigonal or higher symmetry ($\eta = 0$), the powder distribution of the central line is given by[19]

$$f(\nu) = \begin{cases} [(5+3x)^{-1/2} + (5-3x)^{-1/2}]/4x, \\ \qquad \nu_L - 16A/9 \leq \nu \leq \nu_L \\ (5-3x)^{-1/2}/4x, \quad \nu_L \leq \nu \leq \nu_L + A \\ 0 \quad \text{everywhere else} , \end{cases} \quad (2)$$

where

$$x = [16/9 + (\nu - \nu_L)/A]^{1/2} ,$$

and

$$A = \frac{I(I+1) - \frac{3}{4}}{16\nu_L} \left[ \frac{3e^2qQ}{2I(2I-1)h} \right]^2 = \frac{I(I+1) - \frac{3}{4}}{16\nu_L} \nu_Q^2 .$$

If the actual line shape due to the nuclear dipole-dipole interaction is Gaussian with a half width $\sigma$ much smaller than the distance between the singularities of the powder spectrum $\Delta_2$, one can immediately evaluate $A$ and the quadrupole coupling frequency $\nu_Q$. For $I = \frac{3}{2}$ (see inset in Fig. 1) one has

$$\Delta_2 = \frac{25A}{9} = \frac{25\nu_Q^2}{48\nu_L} . \quad (3)$$

The spectra for pyrolitic *h*-BN and for the BN film, obtained from the FT of the FID, are shown in Fig. 1(a). It is noted that the deposition process in the film does not induce sizable variation in the EFG's at the B site. The line corresponds to the central transition with second-order quadrupole broadening. This conclusion is supported by the fact that the correspondent signal was maximized by a pulse length close to one-half of the one maximizing the $^{11}$B NMR signal in a solution of $HBO_3$. The separation between the two peaks, observed at $\nu_L = 21.8$ MHz, was found to be $\Delta_2 = 54 \pm 2$ kHz, practically independent of the temperature in the range 10–430 K. The peak separation $\Delta_2$ becomes $46 \pm 3.5$ kHz at $\nu_L = 24$ MHz and $15.0 \pm 0.2$ kHz at $\nu_L = 80.47$ MHz, inversely proportional to $\nu_L$ as expected from Eq. (3) [see Fig. 1(b)]. The shift of the NMR line with respect to the reference solution turns out to be negligible, supporting the conclusion that an effective field at the $^{11}$B site from the paramagnetic centers is mostly of dipolar origin. In

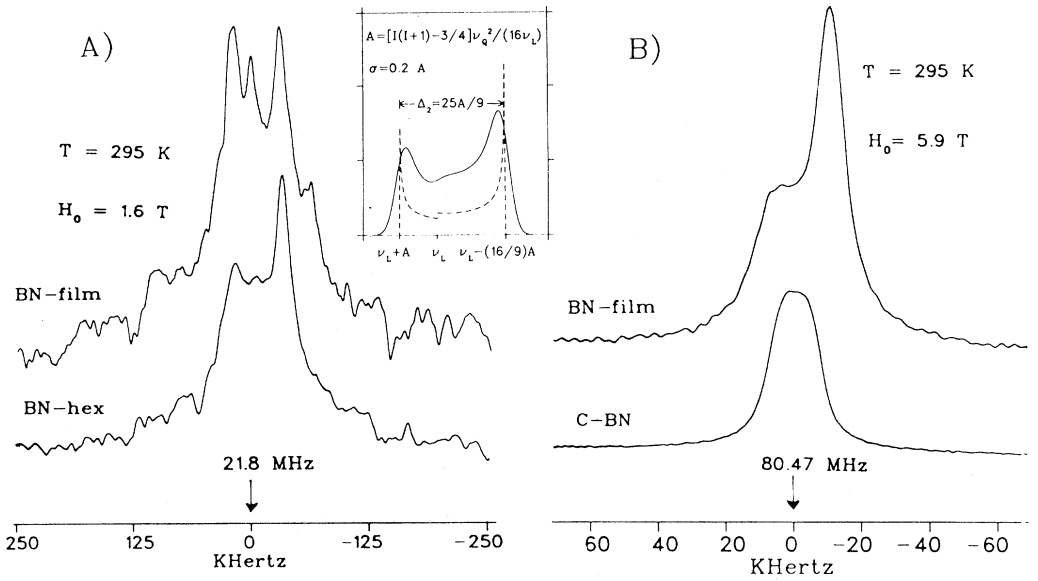


FIG. 1. $^{11}$B NMR spectra for different allotropic forms of boron nitride obtained from FT of the FID signals. BN film and hexagonal BN at 1.6 T (a) the small bump at the resonance frequency (21.8 MHz) corresponds to cubic BN (see text). BN film and the cubic *c*-BN at 5.9 T (b). In the inset the simulated spectrum (continuous line) for a Gaussian dipolar line shape (half width $\sigma=0.2$ A) in the presence of a powder distribution of the second-order quadrupole interaction, as predicted by Eq. (2) in the text (dashed line), is shown.

this case, in fact, the field due to a magnetic moment at position **r** with respect to a nucleus at the origin is

$$\mathbf{h}=-\gamma\hbar\left\{\frac{\mathbf{S}}{r^3}-\frac{3(\mathbf{r}\cdot\mathbf{S})\mathbf{r}}{r^5}\right\}, \tag{4}$$

which yields zero average field $\langle h_z\rangle$ for an isotropic random distribution of $\langle S_z\rangle \propto H_0$. The negligible contribution from the contact term is related to the fact that the nuclei close to the paramagnetic centers are unobservable because of the large NMR shift. In fact, the effective field due to the contact term is $h_e=(8\pi/3)g_e\beta_e S_z|\psi|^2$. The experimental result from EPR (Refs. 15–17) yields $|\psi|^2=1.05\times10^{23}$ cm$^{-3}$, thus implying for the nuclei nearest to the paramagnetic centers a shift of the $^{11}$B NMR frequency around 11 MHz.

The quadrupole coupling frequency for *h*-BN is $\nu_Q=1.50\pm0.05$ MHz, in agreement with previous results.[9] The observed value of $\nu_Q$ in *h*-BN is equal to 55% of that of $^{11}$B for one excess *p* electron $(\nu_Q)_p=2.695$ MHz, measured from the hyperfine structure in atomic beam experiment.[20] Silver and Bray[9] interpreted this result as an indication of a resonating double bond structure with, consequently, a net charge on the boron atom of $-0.45e$. It is now known from theoretical[21–24] and experimental[1,25] studies that the true charge-transfer situation is the opposite: due to the higher electronegativity of nitrogen as compared to boron, a charge transfer, of the order of 0.3–0.5*e* from boron to nitrogen, is expected.

Regarding the intepretation of the EFG, one can remark that the B-N bond has a partial ionic character *i*, and in a crude model this affects the value of *q* for the positive boron ion by the factor $q_{\text{eff}}=(1-i)q_{\text{at}}$. On the other hand, an amount of *s* hybridization increases *q* for the positive boron ion by a factor of $(1+s)$.[26]

The experimental result for *q* should be proportional to $q_{\text{at}}$ due to an electron in the lowest (potentially bonding) *p* state outside the closed electronic shells of an isolated atom,[27] *q* and $q_{\text{at}}$ being related by a proportionality constant determined by the population of the bonding *p* states. For a planar $AB_3$ molecule with the *z* direction perpendicular to the molecular plane the constant is proportional to $K=(n_x+n_y)/2-n_z$, where $n_i$ is the occupancy of the $p_i$ orbital. In the case of pure axially symmetric $sp^2$ bonding, we have for the boron atom $n_z=0$, $n_x=n_y=1$, and therefore $K=1$. From the experimental data one has $K=0.55$. By interpreting this result in terms of a charge transfer from the boron to the nitrogen atom, in agreement with experimental[1,25] and theoretical findings[21–24] and consistent with the electronegativity difference, the net positive charge on the boron atom is $0.45e$ with a reduction of the population of $p_x$ and $p_y$ orbitals. The comparison between the EPR results and theoretical calculations also supports this conclusion.[12]

In the case of polycrystalline cubic BN obtained with the high-pressure and -temperature method, the spectra are shown in Fig. 1(b). No quadrupole interaction is present and the maximization of the signal is obtained with a pulse length about twice that in *h*-BN films. The broadening of the line (FWHI) [full width at half intensity $\Delta=16$ kHz at $H_0\simeq5.9$ T] in *c*-BN samples is larger than the width estimated on the basis of the nuclear dipolar interaction only. The evaluation of the dipolar second moment due to $^{11}$B, $^{10}$B, and $^{14}$N nuclei yields, according to the standard formula,[28] a FWHI $\Delta_{\text{dip}}=9.5$ kHz. The extra broadening probably results mostly from quadru-

pole effects related to the presence of dislocations, local stresses, and defects. In fact, from measurements at different fields a slight decrease of $\Delta$ is observed, consistent with a fraction of about 80% of broadening of quadrupolar origin and 20% of magnetic origin, namely, from the powder distribution of paramagnetic dipolar fields. Finally, from the spectra in Fig. 1(a) for the BN film, one can observe that a small amount of cubic BN is also present, causing the bump at zero frequency and consistent with x-ray-diffraction observations.[18]

## IV. $^{11}$B NUCLEAR RELAXATION RATES

### A. Results

For a relaxation process driven by the time dependence of the quadrupole interaction due to lattice vibrations, the recovery law expected for the $^{11}$B ($I=\frac{3}{2}$) relaxation is

$$y(t)=\tfrac{1}{2}e^{-2W_{Q1}t}+\tfrac{1}{2}e^{-2W_{Q2}t}\ , \tag{5}$$

where the quadrupolar transition probabilities $W_{Q1}$ and $W_{Q2}$ correspond to $\Delta m=1$ and 2 transitions, respectively. In powder samples usually $W_{Q1}\simeq W_{Q2}$ and an exponential recovery is essentially observed.[29]

For a magnetic relaxation mechanism associated with the fluctuations of the effective magnetic field at the nuclear $^{11}$B sites [see Eq. (4)] and in the presence of static quadrupole interaction, the recovery law is given by[30] $y(t)=ce^{-12W_m t}+(1-c)e^{-2W_m t}$, where $W_m$ is the magnetic relaxation transition probability. The constant $c$ is 0.9 for irradiation of the central line with a single rf pulse and $c=0.6$ in the case of irradiations with a rf pulse sequence much longer than $W_m^{-1}$. It should be observed that for a single saturation pulse (i.e., $c=0.9$) the recovery law in the first decade of the measure ($y\geq 0.1$) is approximately exponential with a time constant

$$T_1\simeq(11W_m)^{-1}\ . \tag{6}$$

Only in the second decade ($y\leq 0.1$) is a sizable departure from the exponential recovery noticeable. However, the precise estimate of $y(t)$ in the second decade is hampered by the small difference $m(\infty)-m(t)$, of the order of the noise.

In the $h$-BN sample, with few paramagnetic centers ($N\leq 10^{13}$ cm$^{-3}$), an exponential recovery was observed, yielding a very long relaxation time ($T_1\geq 120$ sec). Both of these features indicate that the relaxation process is driven by quadrupole interaction. The frequency and temperature dependences of the relaxation rate support this conclusion. That is, no $\nu_L$ dependence was observed and we found $T_1^{-1}\propto T^2$, characteristic of a Raman two-phonon relaxation mechanism driven by lattice vibrations.[28]

Relaxation measurements have been carried out also in cubic BN samples with different values of the paramagnetic center concentration $N$. The absence of static quadrupolar interaction (EFG is 0 in cubic symmetry) implies a common spin temperature, and, for magnetic relaxation mechanism, an exponential recovery law with time constant $T_1=(2W_m)^{-1}$. The random distribution of the paramagnetic centers introduces a site-dependent relaxation rate $W_m$.[31–34] At short time one has a fast decrease of $y(t)$, and only after this transient one has an exponential recovery[31–34] yielding the time constant $T_1$. The recovery in cubic BN is similar to that observed in BN films and shown in Fig. 2(a), where the exponential part is well evidenced for $t\geq 1$ sec. As expected, with the increase of the concentration $N$ of paramagnetic centers the relaxation rate is increased: the exponential long-time component yields relaxation times much shorter than the ones in the samples at low concentration (see Table I).

For the BN films a transient in the recovery law at short times is also present. Then the exponential part sets in, yielding a time constant given by $T_1\approx(11W)^{-1}$, as indicated in Eq. (6). The temperature and field dependences of the relaxation rates, extracted from the exponential part of the recovery in a BN film with a concentration of paramagnetic centers $N\simeq 6\times 10^{18}$ cm$^{-3}$, are shown in Fig. 3.

The transient part of the recovery will be discussed in more detail in Sec. IV B. Here we only mention that the

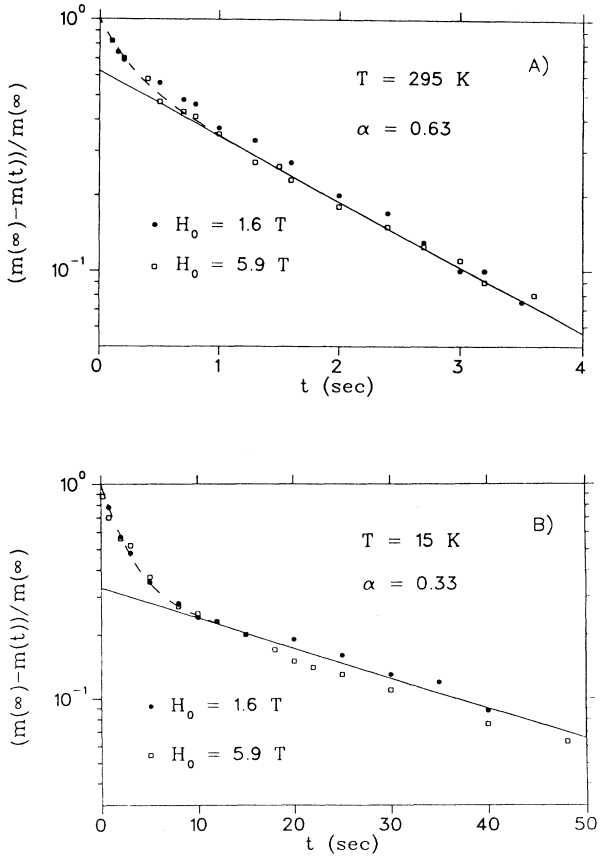


FIG. 2. Recovery of the effective $^{11}$B nuclear magnetization ($+\frac{1}{2}\leftrightarrow-\frac{1}{2}$ central line) for BN film at $T=295$ K (a) and $T=15$ K (b). Open squares (□), $H_0=5.9$ T; closed circles (●), 1.6 T. The solid lines are the best fits for the long-time exponential component ($\alpha$ is the extrapolation at $t=0$).

TABLE I. EPR and $^{11}$B NMR parameters of BN samples (1) at room temperature and $H_0=0.32$ T; (2) at room temperature and $H_0=5.9$ T; (3) translucent BN; and (4) borazon.

| Sample | $g$ value | $N$ (cm$^{-3}$) | $T_{1e}(1)$ ($\mu$sec) | $T_{1n}(2)$ (sec) |
|---|---|---|---|---|
| $h$-BN | 2.0029±0.0004 | $3\times10^{13}$ | 21 | 120 |
| BN film | 2.0026±0.0004 | $6\times10^{18}$ | 16 | 1.8 |
| $c$-BN (3) | 2.0037±0.0004 | $6\times10^{16}$ | 3 | 40 |
| $c$-BN (4) | 2.0039±0.0004 | $4\times10^{19}$ | 2 | 3.7 |

form of the recovery is practically independent of field and temperature, down to $T\simeq50$ K. Below $T\leq40$ K the weight of the exponential part corresponding to the extrapolation at $t=0$ of the long component of the recovery exhibits a rather sharp reduction (see inset in Fig. 3). This effect could be related to the interplay between electronic and nuclear relaxation times: an increase of the $^{11}$B relaxation time can be expected to enlarge the time interval before the occurrence of the exponential recovery.

For the analysis of the experimental results, given in the following subsection, some EPR data (already published elsewhere[15–17]) are recalled here. Except in the case of $h$-BN, where the superhyperfine structure can be resolved, for BN film and for $c$-BN the EPR line is inhomogeneously broadened. The line shape is Gaussian and its width is an order of magnitude larger than that of the single unresolved components as estimated from hexagonal BN. This condition satisfies Castner's assumption[35] in the derivation of the relaxation parameters from the saturation of the $V$-center resonance in alkali halides. Therefore, this procedure has been used in order to derive the electronic spin-lattice relaxation time $T_{1e}$. The relevant EPR results are reported in Table I. In the temperature range 15–300 K, $T_{1e}^{-1}$ in BN film was found to depend linearly on temperature. The value of $T_{1e}$, measured in $Q$ band ($H_0=1.2$ T), is $T_{1e}\sim10^{-6}$ sec, indicating a quadratic field dependence of $T_{1e}^{-1}$. The behavior of the electronic spin-lattice relaxation rate was found to be of the form $T_{1e}^{-1}\propto TH^2$.

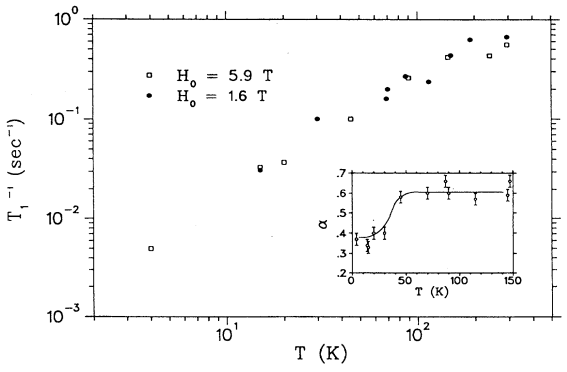


FIG. 3. Relaxation rate $T_1^{-1}\simeq11W$ as obtained from the long-term behavior of the recovery (see Fig. 2) in BN film as a function of temperature (open squares, $H_0=5.9$ T; closed circles, 1.6 T). In the inset the weight of the exponential component of the recovery ($\alpha$ in Fig. 2) is reported.

### B. Analysis and discussion

In the weak-collision approach the nuclear spin-lattice relaxation rate due to the time-dependent part of $\mathcal{H}_{n\text{-}e}$ [Eq. (1)] can be written

$$W_m=\frac{\gamma_n^2}{8}\{J_+(\omega_0)+J_-(\omega_0)\}\ , \tag{7}$$

where $J_\pm$ are the spectral densities for the correlation functions of the transverse components of the effective field $h_\pm$ at the nuclear site [Eq. (4)]. For the fluctuations due to the electronic spin components, by specializing the spectral density[36] and by taking into account the fact that the electronic Larmor frequency is much larger than the nuclear one $\omega_n$ one obtains,[31–34] for the relaxation rate of the nucleus at distance $r$ from the paramagnetic center, the expression

$$2W_m(r)=\frac{2}{5}\frac{\gamma_e^2\gamma_n^2\hbar^2}{r^6}S(S+1)\frac{\tau_c}{1+\omega_n^2\tau_c^2}\equiv\frac{C}{r^6}\ , \tag{8}$$

where $\tau_c=T_{1e}/2\pi$ is an effective correlation time. Due to the inverse sixth-power dependence on the distance, only the nuclei nearest neighbors of the paramagnetic center would have a relaxation rate comparable with the measured one. However, spin diffusion[28,31] acts as an additional mechanism, enhancing the effectiveness of the relaxation process. Thus the nuclear magnetization $M(\mathbf{r},t)$ obeys the equation

$$\frac{\partial M}{\partial t}=D\nabla^2M-\sum_n C|\mathbf{r}-\mathbf{r}_n|^{-6}(M-M_0)\ , \tag{9}$$

where $M_0$ is the equilibrium value in the applied magnetic field and $\mathbf{r}_n$ the position of the $n$th paramagnetic center. The diffusion coefficient $D$ in Eq. (9) is given approximately by $D=a^2/kT_2$, with $a$ lattice constant and $k$ a constant depending on the lattice ($k\sim50$ for a cubic lattice).[31]

The relaxation can be described in terms of four parameters: the internuclear spacing $a$, the average spacing between paramagnetic centers $R\simeq(2\pi N)^{-1/3}$, the pseudopotential radius $\beta$, and the diffusion barrier radius $b$. The field in Eq. (4) affects the Larmor frequency of the nuclei close to the paramagnetic centers, inhibiting the spin-spin transitions with the remaining nuclei.[32] The radius $b$ is the distance at which the magnetic field due to the paramagnetic center equals the local nuclear field

$$b=\left[\frac{3\langle\mu_e\rangle}{\mu_n}\right]^{1/4}a\ , \tag{10}$$

where $\langle\mu_e\rangle$ is the effective electronic moment.[37]

The radius $\beta$ is related to the ratio between the relaxation rate due to the paramagnetic center and the one associated with the nuclear spin diffusion. One has[37] $\beta=(C/D)^{1/4}$. For $\beta$ sufficiently large all the nuclei are practically relaxed by a paramagnetic center. The parameter $\delta=\beta^2/2b^2$ (Ref. 37) can be introduced to identify two different regimes. For $\delta\ll1$ the nuclear relaxation process is driven by the electronic relaxation time (rapid

diffusion). When $\delta \gg 1$ the paramagnetic center releases the energy to the lattice much faster than the process diffusing the nuclear magnetization, and, therefore, the diffusion is the limiting process (diffusion limited). The initial lack of a common spin temperature induces in the nuclear relaxation a transient regime of the order of $C^{1/2}/D^{3/2}$, where the recovery is not described by an exponential law.[32] At longer time the recovery is exponential and a relaxation rate $W$ can be defined. Since the concentration of paramagnetic centers in our samples is such that $\beta \ll R$, each nucleus is under the influence of one paramagnetic center only, and from Eq. (9) one derives[37,38]

$$W = 8\pi N D \beta \frac{\Gamma(\frac{3}{4}) I_{3/4}(\delta)}{\Gamma(\frac{1}{4}) I_{-3/4}(\delta)} , \tag{11}$$

where $I_m = i^{-m} J_m(ix)$ is the modified Bessel function, which in the limiting conditions reads

$$W \approx \frac{8\pi}{3} N \beta D \left[ \frac{\beta^3}{2b^3} \right] = \frac{4\pi}{3} N C b^{-3}, \quad \delta \ll 1 , \tag{12}$$

$$W \approx \frac{8\pi}{3} N D \beta = \frac{8\pi}{3} N C^{1/4} D^{3/4}, \quad \delta \gg 1 , \tag{13}$$

while a transition region occurs for $0.4 \leq \delta \leq 2.0$.

Any attempt to compare the theory and the experimental findings of the nuclear relaxation rate involves knowledge of the concentration and the field and temperature dependence of $T_{1e}$ of the paramagnetic centers. On the basis of Eq. (11), with $D = a^2/50T_2$, $N$ as reported in Table I, $C$ from Eq. (8), and $\tau_c = T_{1e}/2\pi$, with $T_{1e}^{-1} = dTH^2$ (where $d$ is derived from the data at $H_0 = 0.32$ T), one can predict $W$ without adjustable parameters. The comparison between the theoretical prediction and the experimental results for BN film is shown in Fig. 4. One notes that the absolute value of $W$ is well reproduced and the field dependence also appears in qualitative agreement with the overall picture. It is noted that the quasi-independence of $H_0$ is essentially due to a compensation effect. In fact, for slow spin fluctuations (i.e., $T_{1e}\omega_L \gg 1$) one has $W \propto (T_{1e}\omega_L^2)^{-1} \propto (H^{-2}\gamma^2 H^2)^{-1} \equiv \gamma^{-2}$. As regards the temperature dependence, the behavior of the relaxation rate is rather well reproduced for $T \geq 40$ K. A departure seems to occur only in the low-temperature range, where the region of nonexponential recovery appears to increase (see inset in Fig. 3).

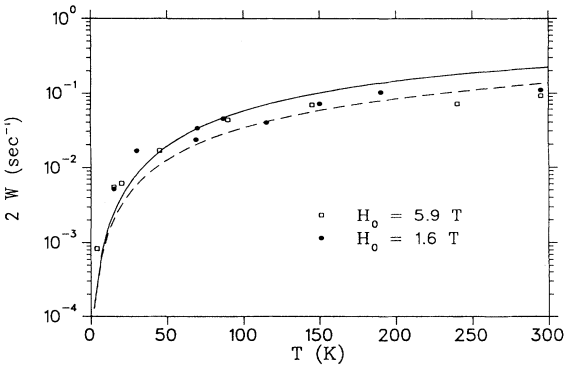


FIG. 4. Comparison of the BN film experimental data for $^{11}$B relaxation rate $2W$ with the theoretical predictions according to the analysis described in the text. The solid and dashed lines are the theoretical behaviors expected for external magnetic fields 5.9 and 1.6 T, respectively.

Finally, a comment on the transient regime of the recovery law is in order. If in the evaluation of the diffusion coefficient $D$ one simply uses $T_2 = 150$ $\mu$sec, then the time interval for the transient $C^{1/2}/D^{3/2}$ is of the order of a tenth of a second, a value considerably smaller than the experimental observation (see Fig. 2). However, one should observe that the effective diffusion coefficient is much smaller than $a^2/kT_2$, since the second-order quadrupole interaction causes a spreading of the $\pm\frac{1}{2}$ Zeeman levels, thus hampering the spin-energy-conserving transitions. By using for $C$ the value $C = 1.26 \times 10^{-42}$ cm$^6$ sec$^{-1}$ (at $T = 100$ K) and by decreasing $D$ by a factor of the order of the ratio of the effective linewidth over the $^{11}$B dipolar one, then one obtains a transient interval of the order of the one experimentally observed. On the other hand, the modification of the effective diffusion coefficient does not affect the estimates of the long-term $W$, since the regime of rapid diffusion is dominating [see Eq. (12)].

## V. CONCLUSIONS

NMR spectra and relaxation measurements in BN films have been used to derive information on the EFG at the B site, the related electronic charge distribution, and the role of the paramagnetic centers (nitrogen vacancies) in driving the nuclear relaxation process. From the quadrupole second-order perturbation of the $^{11}$B Zeeman central line the quadrupole frequency $\nu_Q = 1.5$ MHz has been derived and this result interpreted in terms of charge transfer from boron to nitrogen. While in the case of a small concentration of paramagnetic centers ($N \leq 3 \times 10^{13}$ cm$^{-3}$) the relaxation process is driven by the lattice vibrations through the time dependence of the quadrupole interaction, for a sample with $N \geq 10^{18}$ cm$^{-3}$ it is proven that the dominant relaxation mechanism is driven by the paramagnetic centers assisted by nuclear spin diffusion. A comprehensive explanation of $H$ and $T$ dependence of the $^{11}$B relaxation rates has been given by using for the electronic spin-lattice relaxation time the extrapolation at high field of early EPR results obtained at lower magnetic field. The competition between the spin-diffusion-enhanced relaxation process and the one directly driven by the fluctuation of the effective magnetic moment of the center has been addressed.

## ACKNOWLEDGMENTS

The authors would like to thank Professor A. Rigamonti for his continuous interest and helpful discussions. One of us (M.F.) would like to thank Professor T. D. Moustakas for his support and encouragement. Thanks are due to P. Turella for his help in the measurements. This work was supported by INFM-GNSM, INFN, and the National Science Foundation (Grant No. DMR-9014370).

*Present address: Institute of Physics and Astronomy, Aarhus University, DK-8000 Aarhus C, Denmark.
[1]R. J. Weiss, Philos. Mag. **29**, 1029 (1973).
[2]A. Catellani, M. Posternak, A. Baldereschi, H. J. F. Jansen, and A. J. Freeman, Phys. Rev. B **32**, 6997 (1985).
[3]R. H. Wentorf, J. Chem. Phys. **26**, 956 (1957).
[4]R. M. Chrenko, Solid State Commun. **14**, 511 (1974).
[5]R. T. Paine and C. K. Narula, Chem. Rev. **90**, 73 (1990).
[6]O. A. Galikova, Phys. Status Solidi A **51**, 11 (1979).
[7]S. P. S. Arya and A. D'Amico, Thin Solid Films **157**, 267 (1988).
[8]J. H. Edgar, J. Mater. Res. **7**, 235 (1992).
[9]A. H. Silver and P. J. Bray, J. Chem. Phys. **32**, 288 (1960).
[10]D. Geist and G. Romelt, Solid State Commun. **2**, 149 (1964).
[11]G. Romelt, Z. Naturforsch. Teil A **21**, 1970 (1966).
[12]M. B. Khusidman and V. S. Neshpor, Zh. Eksp. Teor. Khim. **3**, 270 (1967).
[13]M. B. Khusidman and V. S. Neshpor, Fiz. Tverd. Tela (Leningrad) **10**, 1229 (1968) [Sov. Phys. Solid State **10**, 975 (1968)].
[14]A. W. Moore and L. S. Singer, J. Phys. Chem. Solids **33**, 343 (1972).
[15]M. Fanciulli and T. D. Moustakas, in *Wide Band-Gap Semiconductors,* edited by T. D. Moustakas, J. I. Pankove, and Y. Hawakova, MRS Symposia Proceedings No. 242 (Materials Research Society, Pittsburgh, 1992), p. 605.
[16]M. Fanciulli and T. D. Moustakas, Physica B **185**, 228 (1993).
[17]M. Fanciulli, Ph.D. thesis, Boston University, 1993.
[18]T. D. Moustakas, T. Lei, R. J. Molnar, C. Fountzoulas, and E. J. Oles, in *Wide Band-Gap Semiconductors* (Ref. 15), p. 599.
[19]M. H. Cohen and F. Reif, Solid State Phys. **5**, 321 (1957).
[20]G. Wessel, Phys. Rev. **92**, 158 (1953).
[21]C. A. Coulson, L. B. Redei, and D. Stocker, Proc. R. Soc. London Ser. A **270**, 357 (1962).
[22]R. N. Euwema, G. T. Surratt, D. L. Wilhite, and G. G. Wepfer, Philos. Mag. **29**, 1033 (1973).
[23]A. Zunger and A. J. Freeman, Phys. Rev. B **17**, 2030 (1978).
[24]R. Dovesi, C. Pisani, C. Roetti, and P. Dellarole, Phys. Rev. B **24**, 4170 (1981).
[25]G. Will and A. Kirfel, in *Boron Rich Solids,* edited by D. Emin, T. Aselage, C. L. Beckel, I. A. Howard, and C. Wood, AIP Conf. Proc. No. 140 (AIP, New York, 1986), p. 87.
[26]C. H. Townes and A. L. Schawlow, *Microwave Spectroscopy* (McGraw-Hill, New York, 1955).
[27]C. H. Townes and B. P. Dailey, J. Chem. Phys. **17**, 782 (1949); **20**, 35 (1952); **23**, 118 (1955).
[28]A. Abragam, *The Principles of Nuclear Magnetism* (Oxford University Press, London, 1961), p. 112.
[29]A. Rigamonti, Adv. Phys. **33**, 115 (1984).
[30]See T. Rega, J. Phys. Condens. Matter **3**, 1871 (1991); and in particular for $I=\frac{3}{2}$ and magnetic relaxation, F. Borsa, M. Corti, T. Goto, A. Rigamonti, D. C. Johnston, and F. C. Chou, Phys. Rev. B **45**, 5756 (1992).
[31]N. Bloembergen, Physica **15**, 386 (1949); P. G. de Gennes, J. Phys. Chem. Solids, **7**, 345 (1958).
[32]W. E. Blumberg, Phys. Rev. **119**, 79 (1960).
[33]M. K. Cheung and M. A. Petrich, Phys. Rev. B **45**, 9006 (1992).
[34]P. Bernier and H. Alloul, J. Phys. F **6**, 1193 (1976).
[35]T. G. Castner, Jr., Phys. Rev. **115**, 1506 (1959).
[36]C. P. Slichter, *Principles of Magnetic Resonance,* 3rd ed. (Springer-Verlag, New York, 1990), p. 194.
[37]H. E. Rorschach, Jr., Physica **30**, 38 (1964).
[38]G. R. Khutsishvili, Zh. Eksp. Teor. Fiz. **42**, 1311 (1962) [Sov. Phys. JETP **15**, 909 (1962)].